Effects of Mutations on the Thermodynamics of a Protein Folding Reaction: Implications for the Mechanism of Formation of the Intermediate and Transition States †

ARTICLE *in* BIOCHEMISTRY · APRIL 2000

Impact Factor: 3.02 · DOI: 10.1021/bi9923510 · Source: PubMed

4 AUTHORS, INCLUDING:

Jody M Mason
University of Bath
36 PUBLICATIONS **1,251** CITATIONS
SEE PROFILE

Richard Barry Sessions
University of Bristol
182 PUBLICATIONS **4,260** CITATIONS
SEE PROFILE

Effects of Mutations on the Thermodynamics of a Protein Folding Reaction: Implications for the Mechanism of Formation of the Intermediate and Transition States†

Mark Lorch,* Jody M. Mason,‡ Richard B. Sessions,‡ and Anthony R. Clarke‡

IACR-Long Ashton Research Station, Department of Agricultural Sciences, University of Bristol, Long Ashton, North Somerset, BS41 9AF, U.K., and Department of Biochemistry, School of Medical Sciences, University of Bristol, University Walk, Bristol, BS8 1TD, U.K.

Received October 8, 1999; Revised Manuscript Received January 12, 2000

ABSTRACT: We have measured changes in heat capacity, entropy, and enthalpy for each step in the folding reaction of CD2.d1 and evaluated the effects of core mutations on these properties. All wild-type and mutant forms fold through a rapidly formed intermediate state that precedes the rate-limiting transition state. Mutations have a pronounced effect on the enthalpy of both the intermediate and folded states, but in all cases a compensatory change in entropy results in a small net free-energy change. While the enthalpy change in the folded state can be attributed to a loss of van der Waals interactions, it has already been shown that changes in the stability of the intermediate are dominated by changes in secondary structure propensity [Lorch et al. (1999) *Biochemistry 38*, 1377−1385]. It follows that the thermodynamic basis of β-propensity is enthalpic in origin. The effects of mutations on the enthalpy and entropy of the transition state are smaller than on the ground states. This relative insensitivity to mutation is discussed in the light of theories concerning the nature of the rate-limiting barrier in folding reactions.

For single-domain proteins, which fold without the complication of disulfide bond formation and exchange, and where proline isomerization plays no part in the folding reaction, two general patterns of behavior are observed. In the simpler case, the folding reaction is two-state with no populated intermediates prior to the transition state (t-state)[1] (*1* and references therein). In the other case, the reaction is three-state and begins with the rapid formation of a populated intermediate which then slowly converts to the folded state (F-state) by passing through a rate-limiting t-state (*2* and references therein). In general, the larger the protein domain, the more likely it is to fold through a populated intermediate, and it is unclear whether proteins of the two-state variety in fact pass through an intermediate with a free-energy higher than the unfolded state (U-state) so that the I-state is never detected.

The first domain of the cell-surface protein CD2 (CD2.d1) belongs to the three-state category (*3*). The protein is 98 residues in length and composed of two β-sheets arranged in a classical immunoglobulin fold (*4*). There are neither disulfide bonds nor proline isomerizations complicating its folding pathway and folding proceeds through a populated I-state. Several criteria show that the I-state is relatively compact—about 40−45% of core residues are excluded from solvent (*3*, *5*)—and has a well-organized backbone topology in which much of the native conformation is established (*6*, *7*). Mutagenesis demonstrates that interactions between side-chains are extremely weak in the I-state and only become significant in the t-state where a small, but well-defined, nucleus of core residues become organized (*8*). Interestingly, and counter to intuition, thermodynamic measurements on the wild-type protein show that the entropic change from I- to t-state is favorable in the normal temperature range (*5*).

In the work presented here, we extend this thermodynamic examination of the folding reaction by measuring the temperature dependence of folding rates in a series of mutants of CD2.d1. From these data, we extract the enthalpic and entropic effects of the side-chain substitutions on the I-, t-, and F-states. The major reason for undertaking this study is to assess the degree of enthalpy−entropy compensation which, as shown by Shortle and colleagues in equilibrium denaturation experiments, often masks the effects of mutations on the relative free energy of states (*9*).

EXPERIMENTAL PROCEDURES

Source of Protein. All mutants of CD2.d1 were made on the rat gene cloned into the pGEX-2T glutathione-*S*-transferase (GST)-fusion vector (Amersham Pharmacia Biotech). Mutations were generated by the one-sided overlap extension method (*10*) using a Perkin-Elmer DNA thermal cycler. Resulting constructs were transformed into competent *Escherichia coli* HB2151 cells (Amersham Pharmacia Biotech.). Plasmid DNA from transformants overexpressing GST-fusion protein, as assessed by SDS−PAGE, were

† This work was supported by a project grant from the B.B.S.R.C. (U.K.).

* To whom correspondence should be addressed. E-mail: M.Lorch@bris.ac.uk. Phone: 44-(0)117-9287570. Fax: 44-(0)117-9288274.

‡ Department of Biochemistry.

[1] Abbreviations: CD2.d1, domain 1 of the cell surface receptor protein CD2 from rat; GuHCl, guanidine hydrochloride; TEA, triethanolamine hydrochloride; GST, glutathione-*S*-transferase; U-state, unfolded state; I-state, intermediate state; t-state, transition state; F-state, folded state.

10.1021/bi9923510 CCC: $19.00
Published on Web 03/04/2000

prepared and sequenced to check for incorporation of correct mutant codons and to ensure no random errors had been incorporated into the rest of the gene. Oligonucleotides used for mutagenesis and sequencing were obtained from Cruachem Ltd. Sequencing of DNA was performed by the chain termination procedure, using a Du Pont Genesis 2000 automated sequencer.

Wild-type and mutant proteins were prepared and purified as described previously (*3*). Protein concentrations were estimated by UV absorption of aromatic residues at 280 nm [$\epsilon = 5500\ M^{-1}\ cm^{-1}$ for tryptophan (two residues) and 1100 $M^{-1}\ cm^{-1}$ for tyrosine (two residues); for the complete molecule $\epsilon = 13\,200\ M^{-1}\ cm^{-1}$).

Kinetic Folding/Unfolding Measurements. The guanidine hydrochloride (GuHCl) (Sigma Chemical Co.) dependent folding and unfolding rates were measured by fluorescence stopped-flow, as described previously (*3*). Kinetic measurements were carried out in 50 mM triethanolamine hydrochloride (TEA) (Boehringer Mannheim), pH 7.5. Sodium sulfate (Na_2SO_4) (Sigma Chemical Co.) was added to GuHCl and protein solutions at appropriate concentrations to give denaturant activities defined below.

All reaction solutions were maintained at the appropriate temperature using thermostated circulating water baths and were monitored continuously with a sensitive thermocouple. From this, the fluctuation in temperature was determined to be no more than ±0.1 °C.

ANALYTICAL PROCEDURES

Denaturant Activity. A denaturant activity scale in the presence of Na_2SO_4 has been calculated by measuring the free energy of solvation (ΔG_s) of *N*-acetyltyrosine (NAYA) and *N*-acetyltryptophanamide (NAWA) in GuHCl and/or Na_2SO_4 (*6*). For a given concentration of Na_2SO_4, ΔG_s versus GuHCl concentration, for both NAWA and NAYA, can be fitted to the hyperbolic relationship:

$$D = ([\text{GuHCl}]/(K_{den} + [\text{GuHCl}]) + K_{den}\Delta G_{s,0}/(\Delta G_{s,max} - \Delta G_{s,0}) \quad (1)$$

where $\Delta G_{s,max}$ it is defined as the notional, maximum change in free energy of solvation at an infinite GuHCl concentration and a specified Na_2SO_4 concentration, measured relative to water. $\Delta G_{s,0}$ is the change in free energy of solvation, relative to water, at a specified concentration of Na_2SO_4, and in the absence of GuHCl. K_{den} is a denaturation constant and is defined as the concentration of GuHCl required to reach $(\Delta G_{s,max} + \Delta G_{s,0})/2$.

The activity of GuHCl and Na_2SO_4 are both affected by temperature, which is manifested as a change in K_{den} (*5*) (Table 1b). All variables and constants required to convert GuHCl and Na_2SO_4 concentrations to denaturant activity at temperatures between 283 and 318 K are shown in Table 1 and in the table legend.

Treatment of Kinetic Data. The transients of fluorescence intensity (*I*) versus time, which are single, first-order processes, in both the folding and unfolding directions, were fitted to the equation $I = I_a[1 - \exp(-kt)] + I_o$ for rising intensities (where I_a is the fluorescence amplitude of the reaction, *k* is the observed rate constant for the relaxation, and I_o is the initial intensity) and to $I = I_a\exp(-kt) + I_f$ for decreasing intensities (where I_f is the final fluorescence intensity).

Table 1: Variables and Constants Required to Convert GuHCl and Na_2SO_4 Concentrations to Denaturant Activity at Temperatures between 283 and 318 K

(a) Variation of K_{den} with Temperature (*7*)

temp (K)	K_{den}	temp (K)	K_{den}
283	9.67	303	6.78
288	8.95	308	6.05
293	8.22	313	5.33
298	7.50	318	4.61

(b) Variation of $\Delta G_{s,0}$ with Na_2SO_4 Concentration with Temperature (*6*)[a]

Na_2SO_4 concentration (M)	$\Delta G_{s,0}$ (kcal mol^{-1})
0.1	0.09
0.2	0.18
0.3	0.26
0.4	0.34

[a] $\Delta G_{s,max} = -2.43$ kcal mol^{-1} (*6*).

Rate profiles (observed rate constant (k_{obs}) versus denaturant activity) were fitted to the equation (*11*):

$$k_{obs} = k_{F-I} + k_{I-F}/(1 + 1/K_{I/U}) \quad (2)$$

where k_{I-F} and k_{F-I} are rate constants describing the forward and reverse transitions, respectively, between the F- and intermediate (I) states, and $K_{I/U}$ is the equilibrium constant ([I]/[U]) for the rapid interconversion of the I- and U-states. In the fitting routine, the following temporary variables were used:

$$k_{F-I} = k_{F-I(w)}\exp(-m_t D)$$
$$k_{I-F} = k_{I-F(w)}\exp[(m_I - m_t)D]$$
$$K_{I/U} = K_{I/U(w)}\exp[(m_U - m_I)D] \quad (3)$$

where the subscript w describes the rate and equilibrium constants in water, and the *m* parameters describe the shifts in the stabilities of each state (designated by the subscript) as a function of the denaturant activity and have units of molarity^{-1}. These are measured relative to the F-state.

Variation of Free Energy with Temperature. For the variation of the free-energy change associated with a particular transition (ΔG) with temperature (*T*), data were fitted to the following equation (*5*)

$$\Delta G_{(T)} = \Delta H_{(To)} + \Delta C_p(T - T_o) - T\Delta S_{(T_o)} - \Delta C_p T \ln(T/T_o) \quad (4)$$

where $\Delta H_{(T_o)}$ and $\Delta S_{(T_o)}$ are the enthalpy and entropy changes, respectively, at an arbitrarily defined reference temperature (T_o) and ΔC_p is the change in heat capacity (at constant pressure) associated with the transition.

All data were fitted using the Grafit analysis software (Erithracus software, U.K.). When fitting kinetic data to eq 2, proportional weighting was used so that the fitted values took account of rate constants equally across the whole range.

RESULTS AND DISCUSSION

Choice of Mutants. From the set of mutants that were characterized in a previous study (*8*) we selected four to

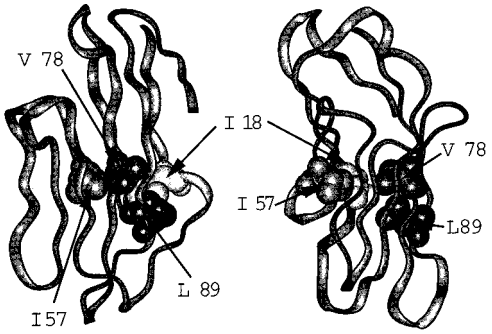

FIGURE 1: Two ribbon diagrams of CD2.d1 (90° rotation relative to one another) with side-chain atoms of residues V78, I18, I57, and L89 shown as spheres.

analyze in greater detail; one mutant that caused a marked increase in stability of the I-state (I57V), one that caused a marked decrease (V78A), and one that caused little change (L89V). The fourth mutant, I18V, was selected so that, along with V78A, the set contained mutations of two of the residues that are involved in the proposed folding nucleus. The postions of the mutated residues within CD2.d1 are shown in Figure 1. All the mutants destabilize the F-state relative to the U-state. Within error, all free-energy measurements are the same as reported in Lorch et. al (*8*). The discrepancy between the thermodynamic parameters for wild-type CD2.d1 reported here and in Parker et al. (5) is due to the different buffers used to carry out the kinetic folding/unfolding experiments. It should also be stressed that all the mutations represent minor truncations of nonpolar, core side-chains and are unlikely to cause widespread structural perturbations.

Increasing Stability of Intermediates. In the case of some mutants, the I-state is only marginally stable. Therefore, a cosmotropic agent, sodium sulfate, has been used to increase the stability of the proteins and thus allowing accurate measurement of the I-state.

The effect of sodium sulfate on the solubility of hydrocarbon has been extensively described in Parker et al. (*6*). Here, it was shown that sodium sulfate acts in an analogous and opposite manner to GuHCl. This effect was quantified and incorporated into the denaturant activity scale described in Parker et al. (*11*), thus extending the scale into negative values in the presence of sodium sulfate.

Treatment of Data. To correct for the nonlinear dependence of the free energy of protein folding on the concentration of GuHCl and Na_2SO_4, observed relaxation rates for folding/unfolding of wild-type and four mutant proteins at different temperatures are plotted against denaturant activity (*D*), as described in analytical procedures (see Supporting Information).

The kinetic data have been fitted to eq 2, which describes a three-state kinetic mechanism (i.e., U to I to F), to yield values for $k_{I-F(w)}$, $k_{F-I(w)}$, $K_{I/U(w)}$, m_U, m_I, and m_t. The fits are shown in the Supporting Information and used to calculate the free-energy changes for each transition. The temperature dependencies of the free-energy changes associated with the equilibrium transitions ΔG_{F-U}, ΔG_{F-I}, and ΔG_{I-U} and kinetic transitions ΔG_{I-t} and ΔG_{t-F} for the four protein's data have been fitted to eq 4 to yield values of ΔH, ΔS, and ΔC_p for the ground and t-states in the folding reactions. These values are shown in Table 2, and illustrated in Figure 2, where ΔC_p is used as a reaction coordinate.

Ground-State Transitions. The clearest observation that can be made concerning the ground-state transitions, i.e., U to I and I to F, is that in all cases $\Delta\Delta H$ is greater than $-\Delta T\Delta S$ (Figure 3). Consequently, the changes in $\Delta\Delta G$ are dominated by enthalpic effects. For all four mutants, there has been an enthalpic destabilization of the overall folding process (U to F), an observation which is explained by a loss of van der Waals interactions in the F-state, which is manifested as a reduction in enthalpy. On average the change in enthalpy caused by the removal of a core methylene group is 3.7 ± 1.8 kcal mol^{-1} compared to change of just 1.7 ± 0.8 kcal mol^{-1} for free energy. This change in enthalpy may appear to be larger than expected for a relatively small loss of contact area, but estimates of the van der Waals contribution to folding enthalpy (*12*) give a value of 2−3 kcal/mol per residue, and it might be expected that internal residues will have a larger contribution than those on the exterior. Moreover, using a standard molecular mechanics force field, the removal of a methane group from the center of a cluster of methane molecules yields a change in potential energy of 2.2 kcal/mol. This value is reasonably close to that measured in our experiments.

When the U-to-F transition is broken down into its two constituent steps, a more complex picture emerges. In the first transition from U to I, the enthalpy change caused by the mutations for I57V, L89V, and, to a lesser extent, I18V is stabilizing, while the opposite is true for V78A. It has already been shown that none of the mutants studied here exhibit any strong native-like side-chain side-chain interactions in the I-state, and in fact, $\Delta\Delta G_{I-U}$ can largely be attributed to changes in β-propensity (*8*). Therefore, it is not surprising that the pattern of enthalpy changes upon mutation seen in the U-to-F transition is not mirrored by the U-to-I transition. Since, in the I-state, mutations to valine from isoleucine and leucine are enthalpically favorable while the opposite is true for the valine to alanine mutation, it follows that valine is enthalpically more favorable than isoleucine, leucine, and alanine. Valine is also a better β-former than isoleucine, leucine, or alanine (*8*, *13*−*18*). This is illustrated in Figure 4 where it is clear that the change in enthalpy upon mutation is of the same sign as the change in β-propensity caused by the mutation. It would therefore appear that the driving force underlying the propensity of an amino acid to form β-structures is enthalpic in nature. This hypothesis is consistent with the main-chain electrostatic model of β-propensities, proposed by Avbelj and Moult (*19*), in which backbone electrostatic interactions are screened by the side-chain between the interacting peptide groups. This model indicates that a change in side-chain would result in different electrostatic interaction energies between neighboring peptide groups, an effect that is expected to be enthalpic in origin.

In opposition to any enthalpic change caused by mutations, there is an entropic change of a similar, but slightly smaller size. This is likely to be due to the fact that the reduction in any stabilizing interactions will result in a less well-defined state, i.e., mutant proteins will not be as tightly packed as the wild-type protein, hence less order will be imposed on the system resulting in a net entropic gain. The result of this "entropy-enthalpy compensation" is a relatively small net change in free energy (Figure 3).

Transition State Barrier. The temperature dependence of free-energy changes associated with the rate-limiting I-to-t

Table 2: Thermodynamic Parameters for the Folding Reactions of wt, I57V, L89V, V78A, and I18V CD2.d1 at 298 K

	U-I	I-F	I-t[a]	t-F[a]
ΔC_p (kcal mol^{-1} K^{-1}) wt	-0.5 ± 0.7	-0.98 ± 0.06	-0.41 ± 0.05	-0.57 ± 0.1
ΔH (kcal mol^{-1}) wt	0.07 ± 0.3	-14.5 ± 0.2	15.9 ± 0.2	-30.3 ± 0.4
$-T\Delta S$ (kcal mol^{-1}) wt	-0.9 ± 0.3	9.2 ± 0.25	-3.2 ± 0.2	12.4 ± 0.4
ΔC_p (kcal mol^{-1} K^{-1}) I57V	-0.28 ± 0.07	-1.58 ± 0.08	-0.60 ± 0.09	-0.90 ± 0.08
ΔH (kcal mol^{-1}) I57V	-1.3 ± 0.3	-11.7 ± 0.3	16.5 ± 0.4	-28.6 ± 0.4
$-T\Delta S$ (kcal mol^{-1}) I57V	0.25 ± 0.3	6.9 ± 0.3	-3.8 ± 0.3	11.1 ± 0.3
ΔC_p (kcal mol^{-1} K^{-1}) L89V	-0.40 ± 0.04	-1.2 ± 0.05	-0.50 ± 0.2	-0.7 ± 0.2
ΔH (kcal mol^{-1}) L89V	-0.6 ± 0.15	-10.7 ± 0.2	15.8 ± 0.7	-26.6 ± 0.7
$-T\Delta S$ (kcal mol^{-1}) L89V	0.25 ± 0.15	5.8 ± 0.20	-2.9 ± 0.7	8.9 ± 0.7
ΔC_p (kcal mol^{-1} K^{-1}) V78A	-0.43 ± 0.04	-1.15 ± 0.7	-0.36 ± 0.05	-0.83 ± 0.06
ΔH (kcal mol^{-1}) V78A	2.2 ± 0.2	-8.5 ± 0.4	14.9 ± 0.3	-23.4 ± 0.3
$-T\Delta S$ (kcal mol^{-1}) V78A	-2.7 ± 0.2	5.5 ± 0.4	-1.3 ± 0.3	6.7 ± 0.3
ΔC_p (kcal mol^{-1} K^{-1}) I18V	-0.65 ± 0.15	-0.85 ± 0.10	-0.20 ± 0.16	-0.64 ± 0.14
ΔH (kcal mol^{-1}) I18V	-0.1 ± 0.7	-8.0 ± 0.5	16.1 ± 0.7	-24.0 ± 0.6
$-T\Delta S$ (kcal mol^{-1}) I18V	-0.8 ± 0.7	3.9 ± 0.5	-3.2 ± 0.7	7.0 ± 0.6

[a] A value for $k'_{(T)}$ of 1×10^{10} s^{-1} was used to calculate $\Delta S^{\ddagger}$. Quoted errors are standard errors calculated from least-squares fits to the data (based on a 95% confidence limit). It should be noted that a weighted nonlinear fit results in an insignificant change in quoted parameters and an increase in the quoted errors of no more than 15%. Accumulated standard errors were calculated using standard statistical formulas.

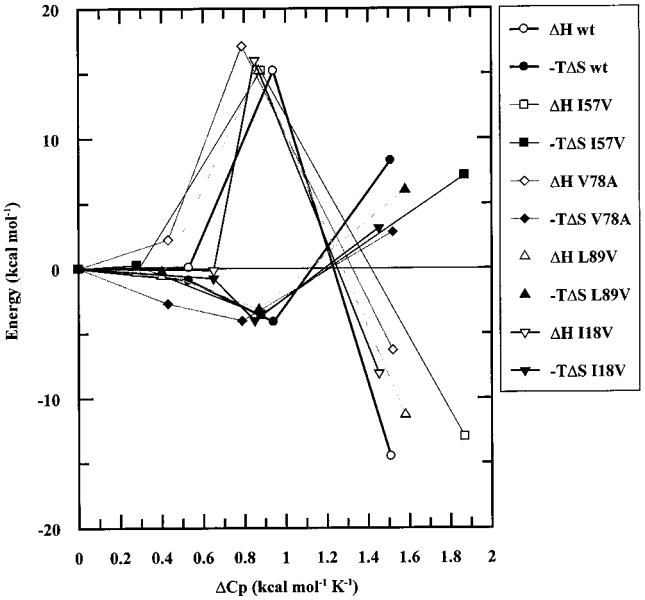

FIGURE 2: Thermodynamic reaction profiles. The enthalpy (ΔH) and entropy ($-T\Delta S$) components of the free-energy changes associated with the U-to-I, I-to-t and t-to-F transitions are plotted against the solvent exposures of the states (ΔC_p), relative to F. Reference temperature (T_o) is 298 K. The activation entropies where calculated using a value of $k'_{(T)} = 1 \times 10^{10}$ s^{-1}.

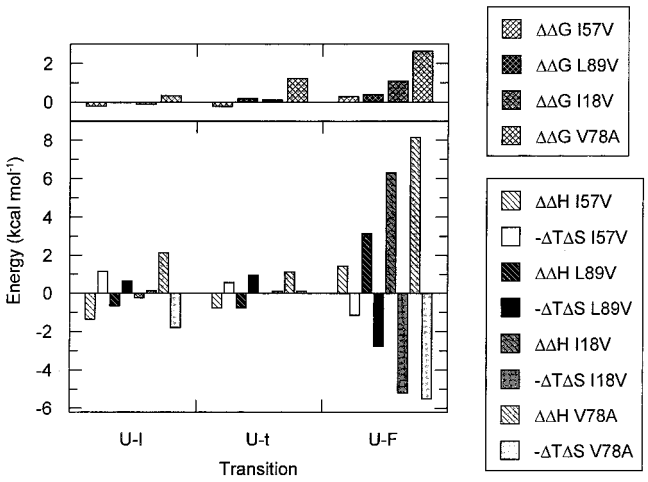

FIGURE 3: Effects of mutations on the energetics of each transition along the folding pathway. Enthalpy and entropy changes ($\Delta\Delta H$ and $-\Delta T\Delta S$, respectively; see Table 2) are shown in the lower part of the graph while free energy changes at 298 K ($\Delta\Delta G = -\Delta T\Delta S + \Delta\Delta H$) are shown in the upper part. Reference temperature (T) is 298 K. The activation entropies are calculated using a value of $k'_{(T)} = 1 \times 10^{10}$ s^{-1}.

($\Delta G^{\ddagger}_{t-I}$) and t-to-F ($\Delta G^{\ddagger}_{F-t}$) transition barriers for wild-type and mutant CD2.d1 are shown in Figure 3. To relate an individual rate constant to the free-energy change of activation ($\Delta G^{\ddagger}$), we use the Eyring equation: $k = k'_{(T)}\exp(\Delta G^{\ddagger}_{(T)}/RT)$, where R is the gas constant and $k'_{(T)}$ is the rate of decay of the activated species, i.e., the rate at which this process would occur in the absence of a free-energy barrier. While the values for the activation enthalpy ($\Delta H^{\ddagger}$) and the activation heat capacity ($\Delta C^{\ddagger}_p$) do not depend on $k'_{(T)}$, the uncertainty in this value precludes an exact evaluation of the activation entropy ($\Delta S^{\ddagger}$). The values of $\Delta H^{\ddagger}$ and $\Delta C^{\ddagger}_p$ calculated for the I-to-t and t-to-F transitions are given in Table 2.

$\Delta S^{\ddagger}$ values for the I-to-t and t-to-F transitions have been calculated using a value for $k'_{(T)}$ at 298K of 10^{10} s^{-1} (based an average "jump time" for a water molecule in *n*-butanol as an approximate mimic of the interior of a partially dehydrated protein (*20*)). These values are given in Table 2. It should be noted that Keifhaber and collegues (*21*) have measured $k'_{(T)}$ experimentally and obtained a value of $\sim 10^8$ s^{-1} at 298 K. While these different values of $k'_{(T)}$ affect the absolute magnitude of $\Delta S^{\ddagger}$, this has no effect on the ensuing arguments.

The mutations cause no major change in the enthalpy and entropy of the t-state. Like wild-type CD2.d1 and N-PGK (*5*) all the mutants, at 298K, have an I-to-t transition that is entropically favorable and enthalpically unfavorable (Figure 2). The heat capacity shows the t-state to be less solvated than the intermediate, hence the origin of the favorable entropy change must lie in the process of water exclusion from hydrophobic surfaces. Only after the t-state barrier is surmounted is there a net entropic penalty arising from the widespread ordering of side-chains in the fully F-state.

Since little is known about the true nature of the t-state, it is difficult to interpret any changes that the mutations might cause. However, upon inspection of the reaction diagram (Figure 2), it becomes apparent that the energetics of the

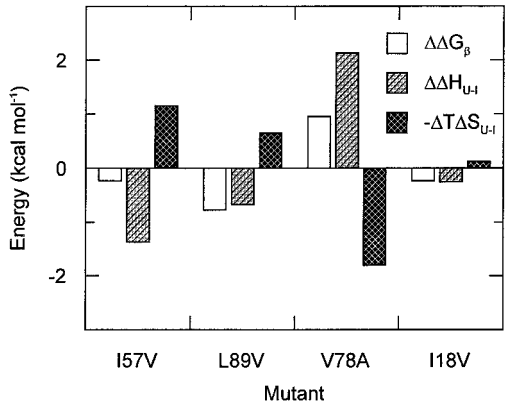

FIGURE 4: Comparison of the changes in entropy and enthalpy of the I-state and changes in β-structure propensity. The difference enthalpy and entropy changes measured for the U-to-I transitions of the mutants I57V, L89V, V78A, and I18V ($\Delta\Delta H_{U-I}$ and $-\Delta T\Delta S_{U-I}$; see Table 2) have been plotted along with the expected difference free energy change due to changes in β-structure propensity [$\Delta\Delta G_\beta$; calculated as described in Lorch et al. (*8*)]. Reference temperature (T) is 298 K.

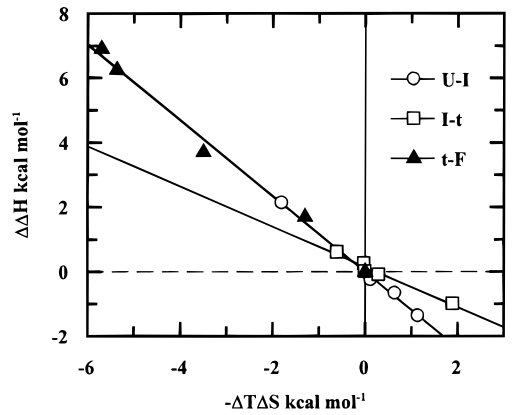

FIGURE 5: Entropy−enthalpy compensation. Data are fitted to a straight line according to the relationship $\Delta H = m \times -T\Delta S + \Delta H_I$, where m is the gradient of the slope and ΔH_I is the intercept with the y-axis. The slopes have gradients of -1.17 ± 0.03 for the U-to-I, and t-to-F transitions and -0.62 ± 0.05 for the I-to-t transition. All fits have a correlation factor of 0.99 or better.

t-state are largely unaffected by the mutations. Within error, the position of the t-states on the reaction coordinate (as measured by the change in heat capacity) are identical, while there is also comparatively little change in the energy of this state. For example, at 298 K, the V78A mutant, which has the most pronounced effect on the energy of the t-state, only alters ΔH_{U-t} by $\sim$2 kcal mol^{-1} compared to a $\sim$7 kcal mol^{-1} change in ΔH_{U-F}. These observations would appear to suggest that the mutations have a larger effect on the stability of the ground states than the t-state. It therefore follows that changes in side-chain interactions between the I- and t-states are relatively unimportant.

Despite the fact that the energetics of t-states are relatively unaffected by mutations, the I-to-t transition still exhibits strong entropy−enthalpy compensation. However, unlike the other transitions, described above, $-\Delta T\Delta S_{I-t}$ is larger than $\Delta\Delta H_{I-t}$. This difference is illustrated in a compensation plot ($-\Delta T\Delta S$ vs $\Delta\Delta H$, Figure 5).

Structural Implications. A major conclusion that can be made from the data presented here concerns the I-to-t transition and the nature of the t-state. It has already been shown that the t-state barrier is enthalpic in origin. Two explanations for this were presented in Parker et al. (*5*). The first model is based on the argument that the I-state is an ensemble of relatively stable misfolded conformations (*22*, *23*). Therefore, non-native interactions that characterize such misfolded states must then be broken before the protein can reach its native conformation. The process of breaking these interactions would incur an enthalpic penalty. Previous studies have shown that the I-state of CD2.d1 exhibits a large amount of native-like backbone hydrogen bonding, though there is little evidence of strong native side-chain side-chain interactions. It therefore remains possible that while the crude conformation of the backbone has formed a native-like topology the side-chains are still in non-native orientations and, consequently, may be forming non-native contacts.

However, if this model is correct then one would expect the following argument to hold true. Since all the mutations studied here reduce the amount of contacts available in the core of the protein, then a mutation would result in there being fewer stabilizing non-native contacts in the I-state. This would results in fewer bonds having to be broken before the protein could proceed to the F-state, consequently, the enthalpic barrier between the I- and F-states would be reduced by mutation. Furthermore, since the enthalpic t-state barrier would be a result of interactions being broken, one would expect the mutations to have a larger effect on the enthalpy of this transition than the entropy (Figure 5). Considering that the mutations cause neither of these effects, it appears that this model is incorrect.

The second explanation for the nature of the t-state barrier is in part derived from the observation that further desolvation of the protein occurs during the I-to-t transition. The model assumes that at some point during the desolvation process water molecules will become isolated from both the bulk solvent and each other. These water molecules would have originated from the first solvation sphere of hydrophobic residues in the I-state, hence there would be little further entropic cost associated with isolating them from other water molecules. The resulting system would be enthalpically unfavorable, as the isolated water molecules would not be fulfilling their hydrogen-bonding potential. However, once the t-state is passed, these trapped water molecules would be released into free solvent and, thus, satisfy their hydrogen-bonding requirements, a process which is enthalpically and entropically favorable. As the native state is approached, docking of side-chains in the core of the protein occurs, a process that is entropically unfavorable but enthalpically favorable. Balancing these factors results in a net gain in enthalpy. If this model were correct, then the main consequences of a truncation mutation would be to reduce the amount of hydrocarbon that requires desolvation. In terms of thermodynamic parameters that describe the I-to-t transition, this would mean an unmeasurably small change in ΔC_p, a small but unfavorable change in entropy, due to the reduced level hydrocarbon that need desolvating, and change in enthalpy to compensate the entropy change. In light of the fact that the heat capacity for the t-state is unaffected by mutation (Figure 3), mutations cause a much smaller change in energy of the t-state than the I- and F-states, and the entropy change caused by mutation is larger than the enthalpy change, this latter model is preferable.

CONCLUSIONS

The results presented here clarify the processes involved in the formation of the I- and t-states. It is clear that the formation of the I-state is driven by β-propensity and that strong side-chain docking has not yet occurred this early in the folding process. Therefore, any changes in the energetics of the I-state must be a result of the changes in β-propensity incurred by the mutation. This correlation suggests that β-propensity is an enthalpic phenomenon as in the electrostatic model of Avbelj and Moult (*19*). Meanwhile, the insensitivity of the t-state to mutation suggests that little side-chain docking is occurring during the I-to-t transition. This coupled with the enthalpic nature of the t-state barrier implies that the barrier is created by the expulsion of water from the core of the protein. We suggest that the t-state barrier is a species containing isolated water molecules, cut off from complete hydrogen bonding. Once this t-state has been surmounted, these water molecules escape into bulk solvent and, subsequently, native side-chain docking occurs.

SUPPORTING INFORMATION AVAILABLE

Two figures of (1) folding dynamics of CD2.d1 and (2) variation of ΔG with temperature equilibrium transitions. This material is available free of charge via the Internet at http://pubs.acs.org.

REFERENCES

1. Jackson, S. E. (1998) *Folding Des. 3*, 81−91
2. Clarke, A. R., and Waltho, J. P. (1997) *Curr. Opin. Biotech. 8*, 400−410.
3. Parker, M. J., and Clarke, A. R. (1997) *Biochemistry 36*, 5786−5794.
4. Driscoll, P. C., Cyster, J. G., Campbell, I. D., and Williams, A. F. (1991) *Nature 353*, 762−765.
5. Parker, M. J., Lorch, M., and Clarke, A. R. (1998) *Biochemistry 37*, 2538−2545.
6. Parker, M. J., Dempsey, C. E., Lorch, M., and Clarke, A. R. (1997) *Biochemistry 36*, 13396−13405.
7. Parker, M. J., Dempsey, C. E., Hosszu, L. L. P., Waltho, J. P., and Clarke, A. R. (1998) *Nat. Struct. Biol. 5*, 194−198.
8. Lorch, M., Mason, J. M., Clarke, A. R., and Parker, M. J. (1999) *Biochemistry 38*, 1377−1385.
9. Shortle, D., Meeker, A. K., and Freire, E. (1988) *Biochemistry 27*, 4761−4768.
10. Horton, R. M., and Pease, L. R. (1991) in *Directed Mutagenesis: A Practical Approach* (McPherson, M. J., Ed.) Chapter 11, Oxford University Press, Oxford.
11. Parker, M. J., Spencer, J., and Clarke, A. R. (1995) *J. Mol. Biol. 253*, 771−786.
12. Makhatadze, G. I., and Privalov. (1993) *J. Mol. Biol. 232*, 639−659.
13. Kim, C. A., and Berg, J. M. (1993) *Nature 362*, 267−270.
14. Minor, D. L., and Kim, P. S. (1994) *Nature 371*, 264−267
15. Minor, D. L., and Kim, P. S. (1994) *Nature 367*, 660−663.
16. Smith, C. K., Withka, J. M., and Regan, L. (1994) *Biochemistry 33*, 5510−5517.
17. Chou, P. Y., and Fasman, G. D. (1978) *Annu. Rev. Biochem. 47*, 251−276.
18. Munoz, V., and Serrano, L. (1994) *Proteins: Struct., Funct., Genet. 20* 301−311
19. Avbelj, F., and Moult, J. (1995) *Biochemistry 34*, 755−764
20. Weast, R. C. (1989) *Handbook of Chemistry and Physics*, 70th ed., CRC Press, Inc.
21. Bieri, O., Wirz, J., Hellrung, B., Schutkowski, M., Drewello, M., Kiefhaber, T. (1999) *Proc. Natl. Acad. Sci. U.S.A. 96*, 9597−9601.
22. Kiefhaber, T. (1995) *Proc. Natl. Acad. Sci. U.S.A. 92*, 9029−9033.
23. Mirny, L. A., Abkevich, V. Shakhnovich, E. I. (1996) *Folding Des. 1*, 103−116.

BI9923510